CO_2 CONCENTRATION PREDICTION WITH HYBRID NEURAL NETWORKS IN TRAINING BOATS

Jesús Cillero-Ares1, Pedro Carrasco-Pena2, Pedro Fernández-de-Córdoba3, Fernanda Peset3, Carlos A. Reyes3 y Alicia V. Carpentier2, 4

1 Armada Española. Arsenal Militar, s/n - 15401 Ferrol, A Coruña (España).

2 Grupo de Matemática Aplicada para la Defensa. Centro Universitario de la Defensa en la Escuela Naval Militar. Plaza de España, s/n - 36920 Marín, Pontevedra (España).

3 Universitat Politècnica de València. Instituto Universitario de Matemática Pura y Aplicada. Camino de Vera, s/n. - 46022 Valencia (España).

4 Universidade de Vigo. Grupo de Ingeniería Física. Campus de As Lagoas - 32004 Ourense (España).

DOI: https://doi.org/10.52152/D11489 | Recibido: 09/jul/2025 • Inicio Evaluación: 10/jul/2025 • Aceptado: 03/oct/2025

To cite this article: CILLERO-ARES, Jesús; CARRASCO-PENA, Pedro; FERNÁNDEZ-DE-CÓRDOBA, Pedro; PESET, Fernanda; REYES, Carlos; CARPENTIER, Alicia. CO2 CONCENTRATION PREDICTION WITH HYBRID NEURAL NETWORKS IN TRAINING BOATS. DYNA January February 2026. Vol. 101, n.1, pp. 69-75 | DOI: https://doi.org/10.52152/D11489

ABSTRACT: This study presents a hybrid neural network architecture incorporating LSTM, CNN and MLP layers for predicting CO_2 concentrations in marine environments. The proposed architecture uses 96 input variables and generates 48 output variables, enabling it to efficiently capture temporal and spatial patterns in the analysed data. Cross-validation with five folds was implemented to assess the generalisability of the previously validated model. Additionally, new time series data from four different locations on three Navy training vessels operating in the same area were incorporated to test the model's performance in real conditions. The statistical techniques applied proved effective and accurate. In training conditions, the model achieved a MAE of 8.5–12.5 ppm and a MAPE of 2–3%, demonstrating its effectiveness in environmental monitoring in training boats.

Keywords: hybrid neural network; maritime environments; prediction of CO_2 concentration; training vessels; model validation and generalisation.

FUNDING

Generalitat Valenciana (Spain) through the Grant PROMETEO CIPROM/2023/32**;** Grant PICUD-2023-04 from the Defence University Centre at the Naval Military School in Marín, Spain; Grant ED431B 2021/22 (Xunta Galicia).

1. - INTRODUCTION

The concentration of carbon dioxide (CO_2) in the marine environment plays a fundamental role in ecological balance and global climate regulation. The increase in CO_2 emissions from anthropogenic activities has raised ocean absorption of this gas, causing seawater acidification and negative impacts on aquatic ecosystems [1-2]. People in enclosed spaces, such as buildings or boats, are exposed to CO_2 concentrations through breathing that can affect health [3]. Accurate monitoring and prediction of CO_2 in marine environments is essential to develop mitigation strategies that counteract adverse effects and improve health conditions in enclosed workspaces on ships and boats [4-7].

The Defence University Centre at the Naval Military School in Marín (CUD-ENM) is the reference centre for the training of Navy officers in Spain. Its staff works in a coastal environment in the north-east of Spain. Students receive their training in classrooms on land, and on board the Navy's training vessels at the Naval Military School (ENM). The CUD-ENM and the ENM offer a unique and suitable environment to carry out this study, due to their infrastructures and context, allowing an effective analysis and prediction study of CO_2 concentrations in maritime environments, as is done in other environments [8-11].

This study and prediction of CO_2 concentrations have implications not only for inner environment control, but also for occupational health and safety through its influence on cognition and work performance [12]. This is particularly relevant for government institutions such as the Navy and other defence bodies, responsible for large numbers of personnel, sometimes for periods of 24/7. The results can serve as basis to develop policies and mitigation strategies to improve working conditions on ships and the resilience of naval operations [13].

Advanced tools are essential for analysing and predicting CO_2 concentrations. Artificial Neural Networks (ANNs), inspired by the human brain, can learn and generalise from data. Recent studies show their applicability in industrial and social contexts [14–17].

ISSN: 0012-7361 eISSN: 1989-1490 / DYNA Vol.XX nºX DOI: https://doi.org/10.6036/XXXX

ANNs consist of interconnected layers that use non-linear activation functions to model complex relationships between input and output variables. In this study, three types of networks are considered at a theoretical level:

1. **Multilayer perceptron (MLP)** is a basic ANN with input, hidden, and output layers. Its activation functions enable the learning of intermediate representations and non-linear relationships between variables [15].
2. **Convolutional neural networks (CNNs)** use convolutional operations to extract local features and spatial patterns, making them effective for tasks such as classification and complex pattern recognition in multidimensional data [16].
3. **Long short-term memory (LSTM)** networks are a recurrent variant designed to capture long-term dependencies in sequential data. Their gating mechanisms regulate information flow, making them suitable for analysing CO_2 time series and capturing temporal patterns [17].

On the other hand, the material on which the analyses are performed is a crucial component. Data lifecycle management (DLM) [18-19] must be considered in the context of ANNs, following different critical phases that ensure the quality and effectiveness of the developed model by seeking data cleansing, normalisation and validation. These phases are:

4. **Data acquisition and pre-processing:** CO_2 data are collected in specific marine environments and pre-processed by cleaning, normalising, and transforming to remove noise, handle missing values, and prepare for training.
5. **Training with validation:** Model weights are adjusted with optimisation algorithms to minimise loss, while validation on unseen data ensures generalisability.
6. **Implementation for model exploitation:** After training and validation, the model is deployed in real environments, integrated into monitoring systems, and used to generate reports for environmental management.
7. **Compliance with norms and standards:** Data management follows international standards for dissemination and re-use, ensuring reliability of results and safeguarding ship environments and crew well-being.

This work explores the determination and prediction of environmental quality in enclosed spaces based solely on CO_2 concentration. The approach relies on a recurrent neural network (RNN) model that performs temporal prediction of environmental conditions using CO_2 as the main input variable.

The article is structured as follows: Section 2 describes data acquisition, preprocessing techniques, and the hybrid neural network; Section 3 covers training and validation with performance metrics; Section 4 presents results with new datasets; and Section 5 provides discussion, conclusions, and future research.

2. - MATERIAL & METHODS

The development of the model used for data analysis was structured into the following phases, which will be broken down into stages. These stages are dealt with separately in sections 2.1 to 2.9:

1. Data acquisition and preprocessing:
   a. Data acquisition: Acquisition and storage of data over an extended period of time to enable training of the neural network.
   b. Data preprocessing: cleaning, normalising and transforming this data.
2. Training with validation:
   a. Architecture design based on a configuration of LSTM, CNN and MLP layers.
   b. Model training for hyperparameter tuning and optimisation.
   c. Cross-validation: evaluation of the model's generalisation capability using 5-fold cross-validation.
3. Implementation for model exploitation:
   a. Evaluation with new data: testing the model under real conditions.
   b. Analysis of results: interpretation of performance metrics.
4. Compliance with norms and standards:
   a. Compliance with norms and standards in terms of safety, information security, and data protection.
   b. Documentation and reporting: preparation of the scientific report on which this article is based.

2.1. DATA ACQUISITION

Data collection was carried out using CO_2 sensors called 'AirQ-Monitor' [20] to monitor environmental variables in enclosed and open spaces. These variables include temperature, relative humidity and occupancy level. The basic components of the system are:

- One SoC (system on a chip) ESP32 (integrated into the PCB), which is the system's main processor.

ISSN: 0012-7361 eISSN: 1989-1490 / DYNA Vol.XX nºX DOI: https://doi.org/10.6036/XXXX

- One SCD30 sensor, which is a module for detecting CO_2 concentration (with an error margin of ±50 ppm), temperature and humidity.
- One 2.4-inch TFT touch screen for displaying and configuring the equipment.

All the sensors that were installed for data collection were connected to a server, where the data was stored. The structure of the sensors and the data collection process can be seen in Figure 1.

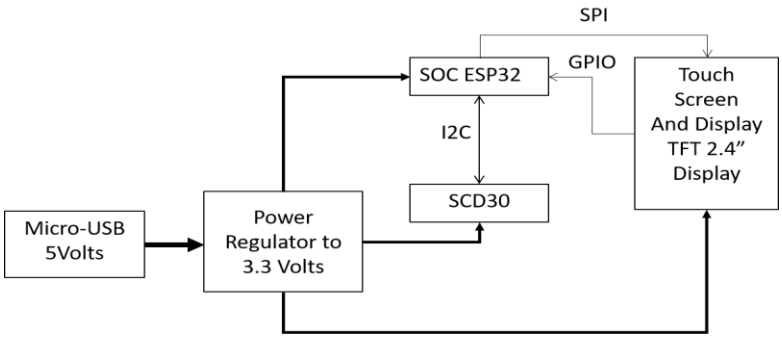


Figure 1. Block diagram of the sensors used.

Figure 2 shows the physical layout of the sensors in the monitored spaces. This article analyses those in the Training Boat Squadron (TBS), labeled CUD-14 to CUD-17, installed on three vessels. The selected Training Boats (TBs) belong to the successful Rodman 66 class, used by public bodies in many countries [21]. These boats conduct training navigation in the coastal environment of the Ría de Pontevedra (Spain). The interior spaces analysed for TB-A and TB-B are identical (Figure 3a). TB-C has a single space (Figure 3b), covering the same volume as the two spaces in TB-A and TB-B.

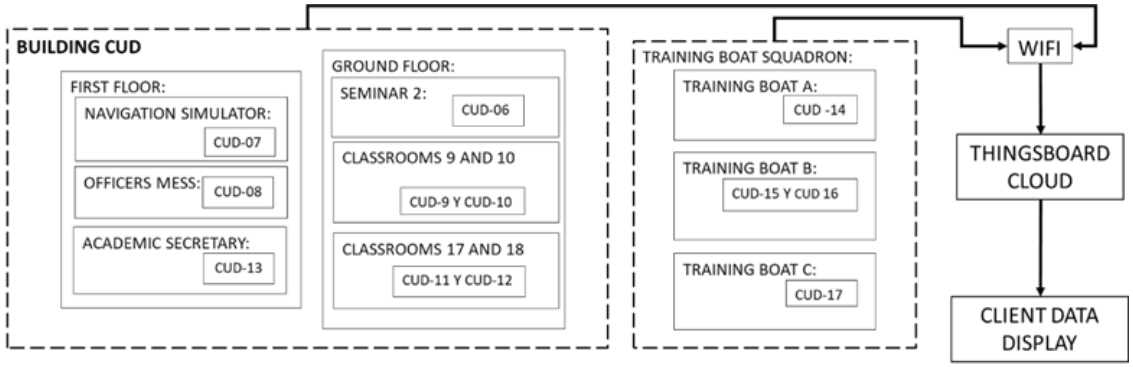


Figure 2. Block structure of the sensors arrangement in the CUD-ENM and the training boats.

ISSN: 0012-7361 eISSN: 1989-1490 / DYNA Vol.XX nºX DOI: https://doi.org/10.6036/XXXX

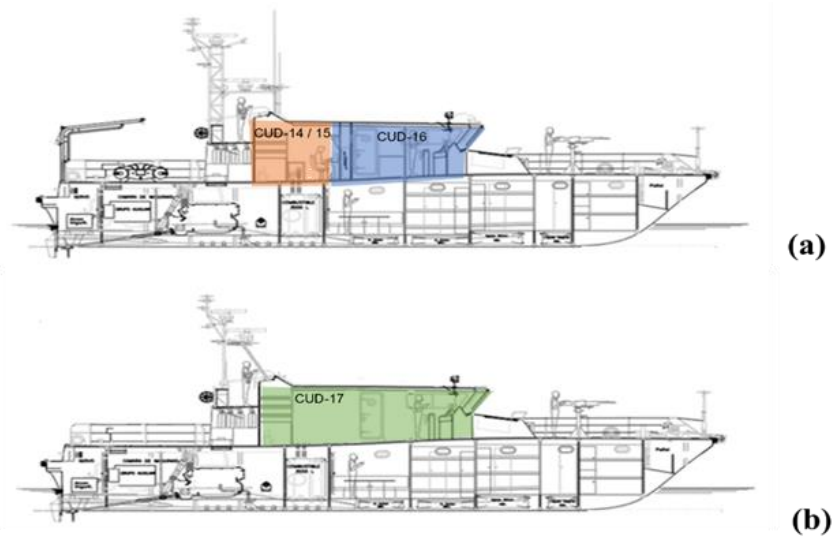


Figure 3. TBs Rodman 66 at the ENM. (a) TB-A and TB-B with sensors CUD-14 to CUD-16. The analysed space is divided into two parts: control center (orange) and bridge (blue). Sensors CUD-14 and CUD-15 were installed in the control center of TB-A and TB-B; CUD-16 in the bridge of TB-B. (b) Sensor CUD-17 was installed onboard TB-C, a single space (green). A Video can be found in the Supplementary Material (Video A1).

The database covers eight months, from June 2024 to January 2025, and was used to train the model and perform cross-validation. Data were split into five folds: in each iteration one-fold was used for validation and the others for training. Loss evolution during training was monitored for each fold.

To assess generalisability, new time series from TB sensors were added. Data from January 2025 tested the model under real operating conditions. The training boats operate in a decentralised coastal environment, mainly in the Pontevedra estuary and adjacent waters (Figure 4).

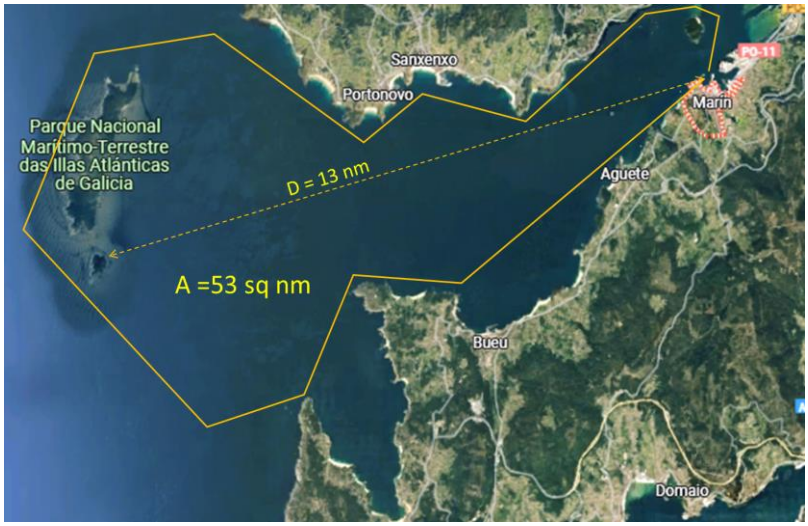


Figure 4. Area where ENM midshipmen train on the boats. It covers 40 sq nm (137 km²) with travel distances up to 13 nm (24 km). (Composition from Google Maps.)

2.2. DATA PREPROCESSING

Data pre-processing involves cleaning, normalising and transforming raw data to remove noise, handle biased or missing values, and prepare it for model training. The model uses periods limited to TB operation, i.e. weekdays from 15:00 to 19:00.

ISSN: 0012-7361 eISSN: 1989-1490 / DYNA Vol.XX nºX DOI: https://doi.org/10.6036/XXXX

Therefore, processing will be restricted to this time series. Although training boats are used at other times, these cases are excluded, since not all boats operate simultaneously, which would add noise and hinder model training.

CO_2 concentration measurements were taken at four locations named Series 14, 15, 16 and 17. Each series contains CO_2 records taken at different times (components). To stabilise the training process and normalise the data ranges, Z-scores were applied according to formula (1) [22].

$$y = \frac{y - \mu}{\sigma} \quad (1)$$

where μ and σ are the mean and standard deviation, respectively, calculated from Series 14. After the prediction is made, the normalisation is reversed in order to calculate the error metrics on the original measurement scale of CO_2 concentrations in parts per million (ppm).

2.3. ARCHITECTURE DESIGN

The network architecture is based on a hybrid model that combines three types of neural network to exploit their individual strengths:

- LSTM: captures complex temporal patterns in the CO_2 series.
- CNN: extracts spatial features and relevant local patterns in the CO_2 series data.
- MLP: processes the output of the previous two layers and generates the final predictions on CO_2 concentration [23].

Figure 5 shows the final architecture of the neural network. This was implemented using a Net Graph in the Wolfram Mathematica environment [24], with each LSTM, CNN and dense layer block connected sequentially and/or in parallel depending on the optimal configuration for the prediction task.

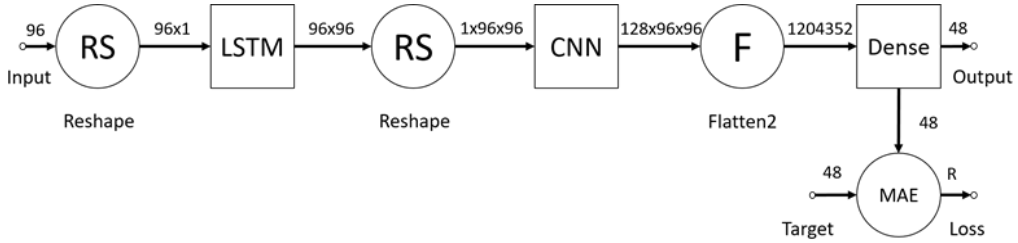


Figure 5. Hybrid neural network with LSTM, CNN, and MLP, showing input and output vectors.

In this network, the inputs, weights and activation functions of each layer are represented by tensors, which can be expressed as follows:

$X \in R^{T \times F}$: The input tensor for CO_2 data in T time steps with F features.

W: The weight matrices at each layer.

b: The biases at each layer.

$\hat{\sigma}$: The activation function (i.e. ReLU, Sigmoid or Tanh).

$Y \in R^{48}$: The output tensor for CO_2 prediction.

For the initial transformation (first reshape), formula (2) represents the values of CO_2 in T time steps and F features.

$$X_{reshaped} = Reshape(X) \in R^{T \times F} \quad (2)$$

The LSTM output is obtained by applying the following recurrent transformation where h_t is the hidden state at time t and c_t is the memory cell state at time t.

$$h_t, c_t = LSTM(X_t, h_{t-1}, c_{t-1}) \quad (3)$$

The LSTM output, represented by formula (4), is the D-dimensional vector h_t.

$$X_{lstm} = h_t \in R^D \quad (4)$$

ISSN: 0012-7361 eISSN: 1989-1490 / DYNA Vol.XX nºX DOI: https://doi.org/10.6036/XXXX

The expression (5) illustrates the transformation of data within the neural network. It indicates that the input tensor (4) is processed to become X_{cnn}, belonging to a vector space with dimensions T (time sequence) and C (channels or features). This notation explains how the form of the data changes as it moves through the network's different layers.

$$X_{lstm} \rightarrow X_{cnn} \in R^{T \times C} \quad (5)$$

Formula (6) describes the process of spatial feature extraction in the CNN. It illustrates how the input tensor (4) is transformed by the application of convolutional weights (W_{conv}), biases (b_{conv}), and an activation function ($\hat{\sigma}$). The result is the output tensor, which captures the extracted spatial features in a vector space dimension of size T×C. In Formula (6), the symbol $*$ denotes convolution.

$$X_{cnn} = \hat{\sigma}(W_{conv} * X_{lstm} + b_{conv}) / X_{cnn} \in R^{T \times C} \quad (6)$$

Formula (7) describes how a multidimensional tensor, X_{cnn}, containing the spatial features extracted by a convolutional layer is converted into a one-dimensional vector, X_{flat}. This vector resides in a D-dimensional vector space and is used by subsequent layers of the neural network, such as fully connected layers.

$$X_{flat} = Flatten(X_{cnn}) \in R^{D} \quad (7)$$

Formula (8) describes how the LSTM output is transformed through fully connected layers (MLP) to generate the final prediction vector. The following steps are then taken in the neural network:

- **First part:** The LSTM output, X_{lstm} is transformed by applying weights and biases, followed by an activation function, to produce X_{mlp}.
- **Second part:** The intermediate result, X_{mlp}, is further transformed using weights, biases and an activation function to produce the final output, Y.
- **Final output:** The final output Y is a 48-dimensional real-space vector (R^{48}) obtained for the case under study.

$$X_{mlp} = \hat{\sigma}\left(W_{mlp} X_{lstm} + b_{conv}\right), Y = \hat{\sigma}\left(W_{cout} X_{mlp} + b_{out}\right), Y \in R^{48} \quad (8)$$

The compact expression for the neural network is obtained by combining all the transformations into a single tensor expression (9).

$$Y = W_{out} \hat{\sigma}\left(W_{mlp} Flatten\left(\hat{\sigma}\left(W_{conv} * LSTM(X)\right)\right) + b_{mlp}\right) + b_{out} \quad (9)$$

This compact expression describes the data flow from input to output in the hybrid neural network.

2.4. MODEL TRAINING

Model training involves adjusting the weights of the neural network using optimisation algorithms to minimise a loss function. Validation involves evaluating the model's performance using data that was not seen during training, thereby ensuring its generalisability.

Series 14 was primarily used to adjust the network weights because more data and relatively stable dynamics were available for this series. Series 15, 16 and 17 were used as validation and test sets to assess the model's generalisability. The network was trained using an Adam optimiser with 50–100 iterations (epochs). This optimiser is widely used in deep learning due to its ability to adapt and handle gradient descent efficiently [25].

The Adam optimiser is an algorithm that updates the weights and biases of a neural network during training. It combines the advantages of the AdaGrad and RMSProp algorithms, making it especially useful for problems involving large datasets and complex parameter spaces, as in this case [26].

Depending on the final version of the network, the main loss function was set as Mean Absolute Error (MAE) or a combination of MAE and Mean Absolute Percentage Error (MAPE). During training, the evolution of the loss in each epoch was monitored, as was the validation metrics, in order to avoid overfitting.

According to formula (10), the MAE value compares the actual (y_i) and predicted ($\hat{y_i}$) CO_2 concentration values (in ppm) for each of the i samples. The MAE value is interpreted directly in units of the variable (ppm).

$$MAE = \frac{1}{N} \sum_{i=1}^{N} \left| y_i - \hat{y}_i \right| \quad (10)$$

According to formula (11), the MAPE value expresses the error in percentage terms. This makes it possible to compare the accuracy of the model against different scales of real values.

ISSN: 0012-7361 eISSN: 1989-1490 / DYNA Vol.XX nºX DOI: https://doi.org/10.6036/XXXX

$$MAPE = \frac{100\%}{N}\sum_{i=1}^{N}\left|\frac{y_i - \hat{y}_i}{y_i}\right| \quad (11)$$

2.5. CROSS-VALIDATION

We use this statistical technique to evaluate model performance and detect overfitting. For each series (14–17), the dataset is divided into folds: in each iteration, one-fold is used to validate the model while the others are used to train it. This is repeated until every fold has served as validation, providing a robust assessment of generalisability. Such validation is particularly relevant to the processes modelled, whose fundamental goal is prediction from the data [27–29].

2.6. EVALUATION WITH NEW DATA

The same evaluation metrics were applied to the new data from the four TB arrangements analysed. This verified the model's ability to generalise and maintain its accuracy under real environmental conditions that were not encountered during training. It should be noted that the model was only trained using time series data on CO_2 concentration (in ppm).

2.7. ANALYSIS OF RESULTS

A comprehensive analysis of the residuals from the hybrid CNN-LSTM model for CO_2 prediction was conducted. The aim was to assess their behaviour under conditions beyond the training set, identifying issues of autocorrelation, component correlation, and variability. This determines the model's applicability to other spaces and time conditions.

2.8. COMPLIANCE WITH NORMS AND STANDARDS

In terms of regulatory compliance, the predictive model was developed in compliance with ethical and legal frameworks for defence-related environments. Because it involves military vessels and personnel, the dataset is subject to confidentiality restrictions imposed by the Spanish Ministry of Defence. Data sharing follows a restricted-access model aligned with national legislation, including the Spanish Law on Science, Technology and Innovation (Law 17/2022), the EU General Data Protection Regulation (GDPR), and occupational safety regulations such as Law 31/1995 on Occupational Risk Prevention. The model also complies with WHO thresholds for indoor CO_2, where concentrations above 1000–1200 ppm indicate poor air quality and occupational risk in confined maritime spaces.

2.9. DOCUMENTATION AND REPORTING

The data management process was documented to ensure reproducibility, including curated datasets and context description. Data access remains restricted by the Ministry of Defence, in line with the regulatory framework outlined above. Long-term preservation and traceability are ensured through RIUNET, the Universitat Politècnica de València's institutional repository, under controlled access.

3. - RESULTS

After training the network with Series 14 and subsequently evaluating the remaining three series, the following error ranges were determined: MAE of 8.5–12.5 ppm and MAPE of 2–3%. This indicates that the network has made stable adjustments with low deviation, which is consistent with this series being the main one used for training.

For validation and test Series 15, capturing CO_2 patterns showed some difficulty, likely due to the surrounding conditions of the analysed space. MAE and MAPE values were 24–55 ppm (sensor error ±50 ppm) and 5–12%, respectively. Although higher than in training Series 14, they still suggest similar pattern behaviour.

In Series 16, pattern capture was also affected by similar environmental factors. Wind, temperature, and occupancy fluctuated between boats, influencing model error. MAE and MAPE values were 21–46 ppm and 4.5–10%. Errors were lower than in Series 15, confirming similarity with Series 14 for training and evaluation.

Finally, in the Series 17 validation and test, it was observed that it was more difficult to capture CO_2 patterns in this boat. This was due to the aforementioned environmental conditions, but also because the configuration of the analysed interior space was different to that of the other boats studied. The MAE and MAPE values were 31–56 ppm and 6.4–12%, respectively.

These results demonstrate that the model can accurately predict CO_2 concentrations in the analysed spaces during cross-validation, indicating the model's generalisability and robustness. These metrics have been shown to be effective in time series prediction competitions such as the M4 Competition [30]. After applying the model to new data (series from January 2025), metrics similar to those obtained during cross-validation were observed, confirming the model's effectiveness in real conditions.

ISSN: 0012-7361 eISSN: 1989-1490 / DYNA Vol.XX nºX DOI: https://doi.org/10.6036/XXXX

MAE and MAPE values remained within acceptable ranges, supporting the model's applicability for continuous CO_2 monitoring in marine environments [31]. Unlike RMSE, MAE does not amplify large errors, making it a robust accuracy indicator for environmental prediction [32–33]. Table 1 summarises the devices installed on the boats and the error values.

Series	MAE (ppm)	MAPE (%)
Series-14 *	8.6-12.5	2-3
Series-15	24-55	5-12
Series-16	21-46	4.5-10
Series-17	31-56	6.4-12

* Training series.

Table 1. This table shows the values for MAE and MAPE errors used to control the model accuracy.

4. - DISCUSSION

The training and validation results show that while the LSTM+CNN model performs well in Series 14, its accuracy decreases in Series 15–17. This underlines the need for representative data from all boats or environments to avoid bias during training. Previous studies indicate that incorporating Big Data techniques into environmental monitoring can yield significant improvements [34].

Another option is to create specific models for each TB or fine-tune the neural network after global training. Prior work has shown this approach to be effective for optimising naval operations [35].

To improve the model's ability to generalise, it is also necessary to explore other variables that could influence CO_2 concentration, such as temperature, occupancy and position.

In conclusion, the LSTM+CNN methodology, with training focused on Series 14 and subsequent evaluation on Series 15–17, confirms the approach's effectiveness in contexts similar to the training series. It also reveals limitations when extrapolating to other environments.

Figure 6 shows the MAE in ppm plotted as a function of the 48 constituents considered. MAE values for constituents in Series 15, 16, and 17 fluctuate compared to those in Series 14. However, these values are relatively low and stable across the range of constituents, as discussed above. This allows us to conclude that the model is valid for analysing and controlling concentrations based on existing regulations [36].

The model's validity can be affirmed in terms of quality and consistency, as the MAE values are sufficiently low and consistent trends are observed. Furthermore, including refinement elements will improve the model, resulting in lower MAE levels. Similar hybrid models have been successfully employed in previous air quality [37] and environmental [36] prediction studies. In particular, these models have been found to be effective for real-time prediction in marine environments [38].

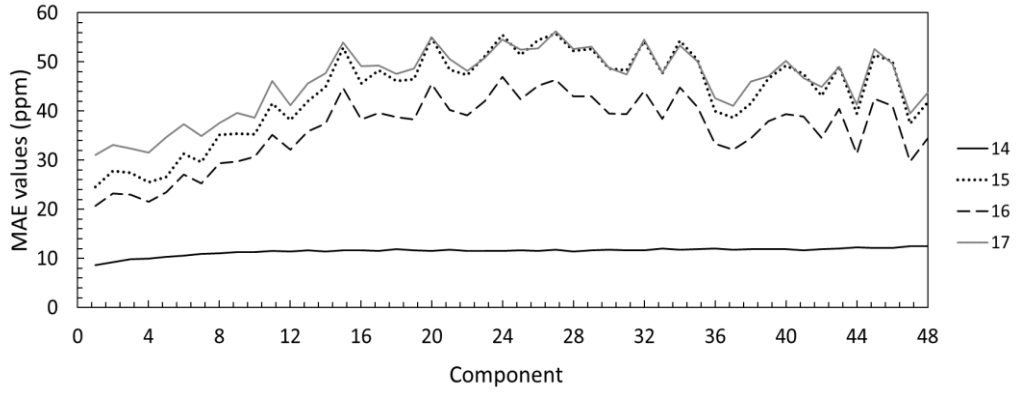


Figure 6. This graph shows the MAE values for each component in ppm. The relevant data can be found in the Supplementary Material (Table A1).

Similarly, Figure 7 shows the MAPE graph. Comparing this with the MAE graph reveals that they both exhibit a similar trend in terms of variability and components, albeit with higher error margins. This affirms the need to revise the model for components with higher errors by adjusting the neural network architecture, incorporating new variables into the training process, or applying optimisation techniques such as fine-tuning. Also, analysing these components in detail will help us determine whether the error differences are

ISSN: 0012-7361 eISSN: 1989-1490 / DYNA Vol.XX nºX DOI: https://doi.org/10.6036/XXXX

due to environmental conditions, sensor limitations or biases in the training data. This could significantly improve the model's generalisability. These aspects naturally lead to a broader discussion on architectures, variables, and transferability.

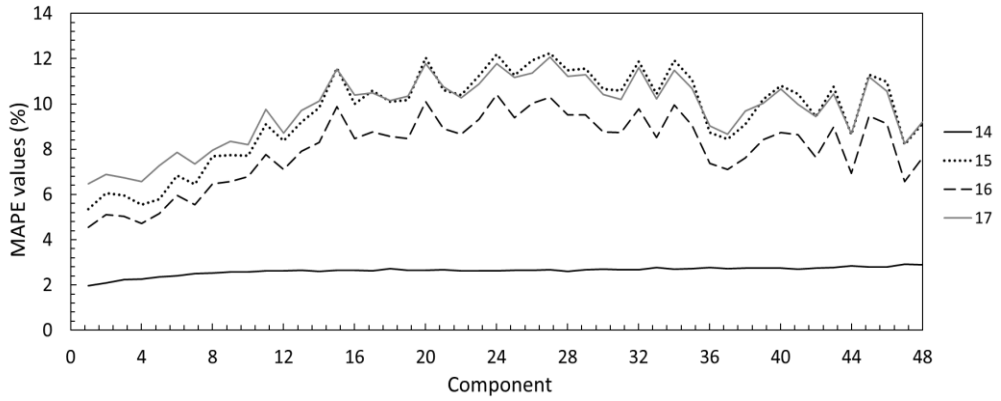


Figure 7. Graph of MAPE values for each of the components in %. The relevant data can be found in the Supplementary Material (Table A2).

Although Transformer architectures are theoretically more powerful than LSTM, they require substantially larger datasets to outperform them. In our context, the limited amount of data led to overfitting during preliminary tests, which supported their exclusion from this study. In contrast, the hybrid LSTM+CNN+MLP achieved the best balance between accuracy and generalisation.

GRU networks were considered as a simplified alternative to LSTM, given their reduced computational complexity. However, in our case, they did not capture long-term dependencies as effectively. For time series such as indoor CO_2 concentrations, the extended memory of LSTM architectures proved more suitable.

Regarding the use of multivariate models, variables such as humidity and temperature were initially considered. However, irregularities in data acquisition (missing values and outliers) reduced their reliability, while their inclusion increased training and preprocessing complexity without proportional performance gains. The univariate approach based solely on CO_2 provided the most efficient and sufficiently accurate solution under the available conditions.

Beyond the ENM training boats, the architecture can be adapted to other naval platforms and civilian environments, requiring only local calibration and enabling integration into IoT and digital twins.

A comparative schematic of the evaluated architectures is provided in Supplementary Figure A1, and their main features and efficiency are summarised in Supplementary Table A3.

The developments described in the article—distributed IoT sensors, an environmental digital twin, and neural networks for CO_2 prediction— align point by point with the Defence Technology and Innovation Strategy (ETID) [39] of the Spanish Ministry of Defense guidelines on digital transformation, sensor exploitation, and AI application. Implementing them on naval platforms or within the Ministry of Defence's infrastructure enhances crew safety and comfort and serves as a showcase for the 4.0 technologies that the Strategy prioritises to achieve operational efficiency and a technological edge.

5.- CONCLUSIONS

The study has enabled the development and validation of a hybrid neural network combining LSTM, CNN and MLP layers for predicting CO_2 concentrations in training ship spaces afloat in the ENM. Cross-validation was implemented for five spaces and new data from four defined positions were evaluated to test the model's performance in real conditions.

The results showed that the model achieved acceptable accuracy in both the cross-validation and the evaluation with new data. The MAE/MAPE metrics demonstrated the model's robust predictive and generalisation capabilities; the initial model over Series 14 achieved an impressive MAPE of just 2–3%, reflecting an excellent fit to the training data.

A reduction in accuracy was observed in Series 15, 16 and 17, with MAPE values between 5% and 12%. This indicates that their representativeness in the training set should be increased. Alternatively, vessel-specific models could be developed to improve fitting to individual scenarios.

In any case, an average MAPE of 8–10% for Series 15–17 may be acceptable for applications where this margin does not affect decision-making. The required accuracy depends on operational needs; for instance, CO_2 thresholds of 1200–1500 ppm in enclosed spaces make such errors tolerable.

ISSN: 0012-7361 eISSN: 1989-1490 / DYNA Vol.XX nºX DOI: https://doi.org/10.6036/XXXX

Accurately predicting CO_2 concentrations in the maritime environment is crucial for monitoring their effects. This study provides an effective, hybrid, neural network-based approach to anticipating changes, which could be useful for risk management and making informed decisions. Using real data from defined spaces located in training boats reinforces the practical applicability of the model in real environmental monitoring situations.

The proposed approach can be extended to other coastal environments, improving understanding of CO_2 effects and supporting mitigation strategies. On Navy vessels, it can be integrated into digital twins for current and future units, offering an effective solution for maritime management with automated variable control and ventilation within the 4.0 environment [40].

This study identified several limitations that should be addressed in future work. For example, real-time sensor data on CO_2 and environmental conditions (e.g. temperature, relative humidity and sea state) should be integrated alongside variables such as changes in crew numbers and HVAC settings. This will improve the accuracy of the model for implementation on IoT devices.

REFERENCES

[1] Chandra Segaran, T.; Nor Azra, M.; Lananan, F.; Youji Wang, Y. Microbe, climate change and marine environment: Linking trends and research hotspots. *Mar. Environ. Res.* **2023**, 189, 106015. https://doi.org/10.1016/j.marenvres.2023.106015
[2] Lu, L.; Chen, H.; Zhang, P. CO_2 Absorption and Its Impact on Marine Systems. *Mar. Chem.* **2022**, 230, 100–110. https://doi.org/10.1016/j.marchem.2021.103892
[3] Lowther, Scott D.; et al. Low-level carbon dioxide indoors—a pollution indicator or a pollutant A health-based perspective. *Environments* **2021**, 8, 125. https://doi.org/10.3390/environments8110125
[4] Mumtaz, R.; et al. Internet of things (Iot) based indoor air quality sensing and predictive analytic—A COVID-19 perspective. *Electronics* **2021**, 10, 184. https://doi.org/10.3390/electronics10020184
[5] Taheri, S.; Razban, A. Learning-based CO2 concentration prediction: Application to indoor air quality control using demand-controlled ventilation. *Build. Environ.* **2021**, 205, 108164. https://doi.org/10.1016/j.buildenv.2021.108164
[6] Wickson, H. Y.; et al. Monitoring of indoor air quality at a large sailing cruise ship to assess ventilation performance and disease transmission risk. *Sci. Total Environ.* **2025**, 962, 178286 https://doi.org/10.1016/j.scitotenv.2024.178286
[7] Ahmed, R., & Tamim, M. T. R. Marine and Coastal Environments: Challenges, Impacts, and Strategies for a Sustainable Future. *International Journal of Science Education and Science.* **2025**, 2 (1), 53–60. https://doi.org/10.56566/ijses.v2i1.325
[8] López, L. R.; et al. CO_2 in indoor environments: From environmental and health risk to potential renewable carbon source. *Sci. Total Environ.* **2023**, 856, 159088. https://doi.org/10.1016/j.scitotenv.2022.159088
[9] Lu, X.; et al. The nexus of the indoor CO_2 concentration and ventilation demands underlying CO_2-based demand-controlled ventilation in commercial buildings: A critical review. *Build. Environ.* **2022**, 218, 109116. https://doi.org/10.1016/j.buildenv.2022.109116
[10] Zahaba, M.; et al. Indoor air quality (IAQ) in a naval ship after refit program: a time variation analysis. *IOP Conf. Ser.: Earth Environ. Sci.* **2022**, 1013, 012004. DOI: 10.1088/1755-1315/1013/1/012004
[11] Zahaba, A.; Gomez, R.; Pérez, L. Monitoring and Training in Naval Environments. *J. Nav. Sci.* **2022**, 5, 20–29.
[12] Satish, U., Mendell, M. J., Shekhar, K., Hotchi, T., Sullivan, D., Streufert, S., & Fisk, W. J. **(2012).**Is CO_2 an indoor pollutant? Direct effects of low-to-moderate CO_2 concentrations on human decision-making performance. *Environmental Health Perspectives, 120*(12), 1671–1677. https://doi.org/10.1289/ehp.1104789
[13] Johnsen, S. O.; Danielsen, BE. Examination of Design and Human Factors Supporting Sensemaking, Resilience and Performance in the Ship Accident Helge Ingstad in Norway. In *Advances in Safety Management and Human Performance,* Proceedings of the AHFE 2021 Virtual Conferences on Safety Management and Human Factors, and Human Error, Reliability, Resilience, and Performance, USA, **2021**. Springer, Cham. https://doi.org/10.1007/978-3-030-80288-2_1
[14] Goti Elordi, A.; Alberdi Celaya, E.; Hernández Guerra, H.; García González, E.; Villar Flecha, J.R.; Sedano Franco, J.; Chira, C. Desarrollo de métodos basados en redes neuronales en la estimación de recursos minerales. *DYNA*, 99(3), **2024**, pp. 263–270. https://doi.org/10.6036/11077
[15] Jaca-Madariaga, M.; Zarrabeitia-Bilbao, E.; Río-Belver, R.-M.; Moens, M.-F. Green Hydrogen: A Social Media Intelligence Analysis. DYNA 2024, 99(3), 250–255. https://doi.org/10.6036/11069
[16] Alonso Mijangos, R.; Saratxaga, E.; Mancisidor, A.; Leizea, I.; Cabanes, I. Intelligent robotic system for automatic identification of marks on parts. *DYNA*, 100(3), 199–203, 2025. https://doi.org/10.52152/D11305
[17] Barajas-Aranda, D.-A.; Torres-Soto, A.; Torres-Soto, M.-D.; Sicilia-Urbán, M.-Á. Comparación y explicabilidad de modelos de aprendizaje automático en el análisis predictivo del suicidio. *DYNA* New Technologies **2024**, 11(1). https://doi.org/10.6036/NT11028
[18] Wang, J.; Xu, C.; Zhang, J.; Zhong, R. Big data analytics for intelligent manufacturing systems: A review. *J. Manuf. Sys.* **2022**, 62, 738–752. https://doi.org/10.1016/j.jmsy.2021.03.005
[19] Gama, J. *Knowledge Discovery from Data Streams*; Boca Raton: FL, USA*: CRC Press*, **2010**.
[20] Reyes Pérez, C. A.; et al. Indoor air quality analysis using recurrent neural networks: a case study of environmental variables. *Mathematics* **2023**, 11(24), 4872. https://doi.org/10.3390/math11244872
[21] Astillero Rodman. Available online: https://rodman.es/producto/nautica-profesional/patrulleras/rodman-66/ (accessed on 7 May 2025).
[22] Zhang, D.; Ding, E.; Bluyssen, P. M. **2022**. "Guidance to assess ventilation performance of a classroom based on CO_2 monitoring". Indoor and Built Environment, 31 (4), 1107-1126. https://doi.org/10.1177/1420326X211058743
[23] Wolfram Research, *Neural Net Repository Documentation,* **2023**. Wolfram Neural Net Repository of Neural Network Models
[24] Kingma, D.P.; Ba, J. A. *A Method for Stochastic Optimization.* In Proceedings of the 3rd International Conference on Learning Representations (ICLR), 2015.
[25] Gentle Introduction to Adam Optimization Algorithm. Machine Learning Mastery, **2021**. Available online: https://machinelearningmastery.com/adam-optimization-algorithm-for-deep-learning/
[26] Yates, L. A.; et al. Cross validation for model selection: a review with examples from ecology. *Ecol. Monogr.* **2023**, 93, e1557. https://doi.org/10.1002/ecm.1557
[27] Bates, S.; Hastie, T.; Tibshirani, R. Cross-validation: what does it estimate and how well does it do it? *J. Am. Stat. Assoc.* **2024**, 119, 1434-1445. https://doi.org/10.1080/01621459.2023.2197686
[28] Ma, M.; et al. A stacking ensemble learning for ship fuel consumption prediction under cross-training. *J. Mech. Sci. Technol.* **2024**, 38, 299-308. https://doi.org/10.1007/s12206-023-1224-9

ISSN: 0012-7361 eISSN: 1989-1490 / DYNA Vol.XX nºX DOI: https://doi.org/10.6036/XXXX

[29] Makridakis, S.; Spiliotis, E.; Assimakopoulos, V. The M4 Competition: Results, Conclusions and Implications for the Future of Forecasting. *Int. J. Forecast.* **2022**, 38, 54–74. https://doi.org/10.1016/j.ijforecast.2021.11.002
[30] Dalal, S.; Kumar, P.; Patel, M. Enhanced CO_2 Prediction Using Hybrid Neural Networks. *IEEE Trans. Neural Netw. Learn. Syst.* **2024**, 35, 234–242. https://doi.org/10.1109/TNNLS.2023.3145678
[31] Chai, T.; Draxler, R.R. Root Mean Square Error (RMSE) or Mean Absolute Error (MAE)? Arguments Against Avoiding RMSE in the Literature. *Geosci. Model Dev.* **2014**, 7, 1247–1250. https://doi.org/10.5194/gmd-7-1247-2014
[32] Hyndman, R.J.; Koehler, A.B. Another Look at Forecast Accuracy Metrics. *Int. J. Forecast.* **2021**, 37, 332–343. https://doi.org/10.1016/j.ijforecast.2020.11.001
[33] Wang, X.; Li, Y.; Zhang, Q. Big Data Analytics in Marine Environmental Monitoring. *IEEE Access* **2022**, 10, 12345–12353. https://doi.org/10.1109/ACCESS.2022.3145679
[34] Hu, Y.; Wang, Z.; Li, X. Risk Management in Maritime Operations Using Machine Learning. *Ocean Eng.* **2021**, 234, 112–121. https://doi.org/10.1016/j.oceaneng.2021.109123
[35] Sharma, R.; Gupta, P.; Verma, M. A. Hybrid Neural Network Approach for Environmental Prediction. *Environ. Model. Softw.* **2022**, 135, 105–113. https://doi.org/10.1016/j.envsoft.2021.105113
[36] World Health Organization (WHO). Available online: WHO guidelines for indoor air quality: selected pollutants. (accessed on 8 May 2025)
[37] Gupta, A.; Kumar, S.; Singh, P. Hybrid Deep Learning Models for Air Quality Forecasting. *IEEE Trans. Sustain. Comput.* **2022**, 7, 200–210. https://doi.org/10.1109/TSUSC.2021.3050281
[38] Yousif, M.T.; Hussein, A.H.; Yousif, S.K. Real-Time CO_2 Monitoring in Marine Vessels Using Deep Learning Techniques. *IEEE Access* **2024**, 12, 789–798. https://doi.org/10.1109/ACCESS.2023.3145680
[39] General Directorate for Armament and Materiel. *Defence Technology and Innovation Strategy 2020.* NIPO 083-21-121-5. Available online: https://publicaciones.defensa.gob.es/defence-technology-and-innovation-strategy-etid-2020-libros-pdf.html (accessed on 30 May 2025)
[40] Kaur, P.; Singh, S.; Kaur, R. Digital Twin Approaches for Maritime Operations: A Comprehensive Review. *J. Mar. Sci. Eng.* **2023**, 11, 815–830. https://doi.org/10.3390/jmse11050815

ISSN: 0012-7361 eISSN: 1989-1490 / DYNA Vol.XX nºX DOI: https://doi.org/10.6036/XXXX

SUPPLEMENTARY MATERIAL

This material provides additional information supporting the main article *"CO_2 Concentration Prediction with Hybrid Neural Networks in Training Boats."* It includes extended datasets, detailed Tables, and supplementary Figures referenced in the manuscript. The material is intended to ensure transparency, reproducibility, and to offer readers deeper insights into the data acquisition process, model validation, and performance metrics.

Supplementary Figure

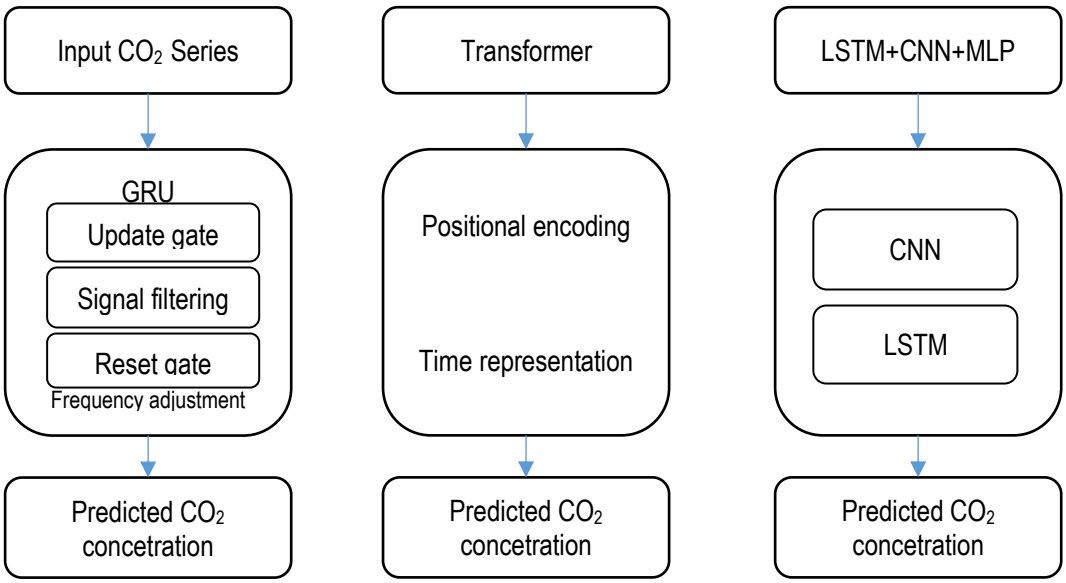


Figure A1.- Comparative schematic of three neural network architectures applied to CO_2 prediction. The diagram contrasts the processing flow of GRU, Transformer, and the hybrid LSTM+CNN+MLP used in this study. Each architecture receives CO_2 time series data as input and applies different mechanisms—gated recurrence, attention with positional encoding, or a hybrid sequence of convolutional, recurrent, and fully connected layers—to generate the predicted CO_2 concentration.

Supplementary video

The video shows the sea trials of two Rodman 66 class Spanish Navy training boats conducted in December 2020 in the Vigo Estuary. The footage documents different operational conditions—including departure from port, low-speed navigation, full-speed trials, and stationary manoeuvres—providing a visual reference of the vessels used in the study.

Supplementary Video A1. Sea trials of Spanish Navy training boats (Rodman 66 class) in the Vigo Estuary. Available at:
https://www.youtube.com/watch?v=ETVIkyfLbW8&list=PL165Lur1CczB6XIDmfcbQvI1ZRU_AV5rY&index=14

ISSN: 0012-7361 eISSN: 1989-1490 / DYNA Vol.XX nºX DOI: https://doi.org/10.6036/XXXX

Supplementary Tables

Component	Series 14	Series 15	Series 16	Series 17
1	8,65856034	24,54195616	20,69996744	31,00520599
2	9,20833149	27,79851444	23,22864793	33,06147542
3	9,85617736	27,41084303	22,97243611	32,33081838
4	9,92375651	25,50842202	21,55456565	31,53496986
5	10,34791227	26,60305931	23,45256590	34,71463183
6	10,57060845	31,29157322	27,05631328	37,38294470
7	10,96362568	29,61641997	25,22181156	34,97496863
8	11,08413046	35,18735444	29,38276517	37,52038491
9	11,24113423	35,45496085	29,77498575	39,56869385
10	11,28515218	35,26889260	30,73058406	38,67975570
11	11,51242329	41,59974304	35,16260282	46,08723637
12	11,46233880	38,22752628	32,17403470	41,17823699
13	11,59598979	42,03871480	35,82540671	45,70651290
14	11,35633619	44,92709174	37,48574538	47,67691988
15	11,64294047	52,85954880	44,62570015	53,92292432
16	11,68874124	45,70308514	38,28848615	49,13882454
17	11,48490822	48,28134491	39,61171371	49,29578548
18	11,94583032	46,11637739	38,77994332	47,56916494
19	11,59746400	46,43211716	38,26026670	48,65343650
20	11,57130600	54,90984627	45,55268379	54,99511430
21	11,76117740	48,45219929	40,18954124	50,60086380
22	11,51676376	47,38018597	39,18221518	48,14369507
23	11,47985132	51,24585083	42,07505736	50,80842456

ISSN: 0012-7361 eISSN: 1989-1490 / DYNA Vol.XX nºX DOI: https://doi.org/10.6036/XXXX

24	11,52060189	55,53979359	46,97822019	54,58711435
25	11,59883781	51,38404177	42,37835881	52,51258086
26	11,57571323	54,38717677	45,21267681	52,77422273
27	11,76965492	55,81504507	46,38301832	56,19965755
28	11,37159204	52,33632860	42,94849148	52,59166408
29	11,60126659	52,68030395	43,00126391	53,10679251
30	11,76577981	48,60906108	39,54791417	48,77400188
31	11,69078001	48,33181283	39,42981590	47,41441990
32	11,70772865	54,18909886	44,03695989	54,52027729
33	12,01877749	47,66687788	38,42857452	47,78537220
34	11,79803985	54,31154059	44,82833921	53,38286477
35	11,85449166	50,48551719	40,84061268	50,09016983
36	12,01396580	39,95538234	33,36741929	42,68881111
37	11,83121241	38,68957688	32,14439469	41,08751697
38	11,87208022	41,60884704	34,43001761	46,01585219
39	11,85039353	46,56658174	37,95022113	47,06305052
40	11,84062936	49,29077569	39,41740468	50,18552160
41	11,67619343	47,62254100	38,94521601	46,74139811
42	11,87601316	43,16161035	34,50402297	44,90770499
43	12,01170970	49,10531826	40,43140470	48,99202249
44	12,29323346	39,50895516	31,35847443	41,36006329
45	12,14065843	51,46987568	42,55226490	52,59886908
46	12,10417644	50,12518377	41,08028620	49,63660449

ISSN: 0012-7361 eISSN: 1989-1490 / DYNA Vol.XX nºX DOI: https://doi.org/10.6036/XXXX

47	12,53471710	37,50054145	29,76866533	39,54126080
48	12,48936495	41,75267087	34,39690596	43,69587675

Table A1. This table shows the values for MAE graph.

Component	Series 14	Series 15	Series 16	Series 17
1	1,97348795	5,34062886	4,54336412	6,45858955
2	2,09363514	6,05915900	5,10314259	6,87890406
3	2,24300182	5,97016105	5,04207574	6,74716987
4	2,25973759	5,55040124	4,72586400	6,57540920
5	2,35472521	5,79021496	5,15484567	7,27708316
6	2,41136226	6,82725083	5,95941518	7,86410713
7	2,50095140	6,45506925	5,54232771	7,34212903
8	2,52894564	7,68674454	6,47310463	7,95192098
9	2,56993145	7,74570363	6,56123736	8,35180252
10	2,57215775	7,70418225	6,77606980	8,20433295
11	2,61923464	9,10518587	7,76937403	9,74798952
12	2,61488064	8,35759466	7,09491985	8,70612374
13	2,65136017	9,19997200	7,91405059	9,71913292
14	2,58972345	9,84011816	8,28608952	10,11706283
15	2,64639023	11,59462423	9,89072316	11,53383423
16	2,65987864	10,009787717	8,46928996	10,39502996
17	2,61970666	10,580440500	8,76254866	10,49551897
18	2,71891118	10,100032177	8,57460957	10,13666936
19	2,64337563	10,171196966	8,46769424	10,34426780
20	2,63799425	12,047155744	10,103273988	11,767418488
21	2,68200856	10,616995466	8,89407704	10,765189922
22	2,63522567	10,380336244	8,66980312	10,279750777
23	2,61882958	11,235584388	9,32131741	10,867935117

ISSN: 0012-7361 eISSN: 1989-1490 / DYNA Vol.XX nºX DOI: https://doi.org/10.6036/XXXX

24	2,62987665	12,18606526	10,42161721	11,77172077
25	2,64050508	11,26593181	9,38987885	11,16862841
26	2,64967451	11,93033150	10,03389084	11,35590337
27	2,68155937	12,24577684	10,28541713	12,06091194
28	2,59989910	11,47638463	9,52237561	11,21277357
29	2,66566288	11,55226438	9,52546694	11,28244776
30	2,69171036	10,65008074	8,75695736	10,40568195
31	2,67183434	10,58847561	8,74042834	10,18791169
32	2,68264667	11,88527057	9,77493664	11,60383075
33	2,77690271	10,44184126	8,51574917	10,21961846
34	2,70173139	11,91214418	9,95021857	11,47462372
35	2,71922032	11,06458007	9,05856750	10,67781736
36	2,78181737	8,73410804	7,37963449	9,03724393
37	2,72597270	8,45349890	7,10602181	8,66305270
38	2,74337806	9,09979709	7,61313722	9,67363608
39	2,73689368	10,19710231	8,41043039	10,01595089
40	2,73636424	10,80073202	8,74426312	10,65284251
41	2,68965854	10,43037830	8,63869471	9,97659891
42	2,73902512	9,44287869	7,63578877	9,43956699
43	2,75837532	10,75833590	8,97542155	10,42931974
44	2,84955938	8,63377623	6,92594364	8,69331070
45	2,78693405	11,28182885	9,45347451	11,19202853

ISSN: 0012-7361 eISSN: 1989-1490 / DYNA Vol.XX nºX DOI: https://doi.org/10.6036/XXXX

46	2,78827033	10,98307809	9,12183257	10,56967143
47	2,90610896	8,18847411	6,57127040	8,24982812
48	2,88971426	9,12916122	7,62064436	9,19433892

Table A2. This table shows the values for MAPE graph.

ISSN: 0012-7361 eISSN: 1989-1490 / DYNA Vol.XX nºX DOI: https://doi.org/10.6036/XXXX

Feature	GRU	LSTM	Transformer
Type	Recurrent (with gates)	Recurrent (with memory cells)	Attention-based (non-recurrent)
Dependencies	Short–medium term	Short–long term	Long-term, global
Complexity	Low–medium	Medium	High
Data requirements	Moderate	Moderate	Very large
Training speed	Fast	Moderate	Slow (but parallel)
Recommended use	Small/medium time series	Time series with long dependencies	Large sequential datasets
Efficiency in this study	Lower accuracy than LSTM	Best trade-off between accuracy and generalisation	Overfitted due to limited dataset

Table A3. Comparative features of GRU, LSTM, and Transformer architectures.

ISSN: 0012-7361 eISSN: 1989-1490 / DYNA Vol.XX nºX DOI: https://doi.org/10.6036/XXXX